Magnetic Field Pitch-Angle Measurements in the PBX-M Tokamak Using the Motional Stark Effect

F. M. Levinton
Plasma Technology Division, JAYCOR, 3547 Voyager Street, Torrance, California 90503

R. J. Fonck, G. M. Gammel, R. Kaita, H. W. Kugel, E. T. Powell, and D. W. Roberts
Princeton Plasma Physics Laboratory, Princeton, New Jersey 08543
(Received 23 February 1989)

Polarimetry measurements of the Doppler-shifted H_α emission from a neutral hydrogen beam on the PBX-M tokamak have been employed in a novel technique for obtaining $q(r)$ and magnetic field pitch-angle profiles using the Stark effect. The resulting $q(r)$ profile is very broad and its central value, $q(0)$, is significantly below 1, which has important implications for theoretical models of sawteeth.

PACS numbers: 52.70.Ds, 52.55.−s, 52.70.Kz

The current-density profile and the safety factor, $q(r)$, are important in the theoretical modeling of plasma equilibrium, stability, and confinement. Many observed phenomena, however, are not well understood due to the lack of consistent and detailed experimental data. For example, current-driven instabilities have been observed or predicted under various conditions, and are known to affect plasma confinement and transport. Since such discharges generally involve auxiliary heating, $q(r)$ measurements in the past have not been available in the resulting high-density plasmas. In addition, when $q(0) < 1$, models predict the plasma to be unstable to resistive kink modes, which are believed to be responsible for sawtooth oscillations in the central temperature. Several theoretical models have been proposed to explain these observations, but to distinguish between them, a detailed knowledge of the safety-factor profile evolution is needed, including evidence beyond experimental uncertainty for a drop in the central $q(0)$ below unity. There are many other instability issues related to the current or $q(r)$ profile, such as the understanding of ballooning or fishbone modes, that could be resolved with detailed profile information.

Techniques for active control of the current density, and the $q(r)$ profile by using rf, neutral beams, or other means are presently underway or being planned. To understand the effects of modifying current-density profiles on stability, confinement, and transport, a credible means of measuring the poloidal field distribution is necessary. Here again, such techniques must be operable in high-density, auxiliary-heated plasmas that are at or near the reactorlike parameters of the present generation of fusion devices.

To date, methods for obtaining current-density and safety-factor profiles have suffered from several problems. Frequently, the measurement is line integrated, which requires a numerical inversion process to obtain spatial information.[1,2] This introduces some uncertainty, particularly for noncircular plasma shapes. Neutral-beam probe techniques have shown good spatial resolution, but so far suffered from beam attenuation for densities above $\sim 1\times 10^{13}$ cm^{-3}.[3,4]

In this Letter we report the first measurements of the central rotational transform, $q(0)$, using the motional Stark effect (MSE) to polarize the spectral emission from a 55-keV neutral-hydrogen beam. One of the principal advantages of this technique is that it can provide a local (~1-2-cm resolution) and highly accurate measurement of the pitch angle of the magnetic field, $\gamma_p(r) = \tan^{-1}[B_p(r)/B_T(r)]$, where B_T is the toroidal magnetic field and B_p is the poloidal field in the midplane. The pitch angle is related to the safety factor, $q(r) = r/R \tan[\gamma_p(r)]$. The safety factor at the magnetic axis ($B_p = 0$), for a circular plasma, is

$$q(0)_{\rm cyl} = \frac{1}{R\, d[\tan(\gamma_p)]/dr\,|_{r=0}}.$$

Another important feature of this method is that beam attenuation is minimal for a hydrogen beam of ~50–80 keV at the operating densities of present-day tokamaks, and hence, this approach extrapolates favorably for use at higher densities and/or in larger machines.

As a neutral beam propagates through a plasma, collisions of the beam particles with the background ions and electrons will excite beam atoms, leading to emission of radiation. In addition, the motional Stark effect,[5] which arises from the electric field induced in the atom's rest frame due to the motion across the magnetic field ($\mathbf{E} = \mathbf{V}_{\rm beam} \times \mathbf{B}$), causes both a wavelength splitting of several angstroms and polarization of the emitted radiation. The $\Delta m = 0$ transitions, or π lines, are linearly polarized parallel to the electric field and the $\Delta m = \pm 1$ transitions, σ lines, are linearly polarized perpendicular to the electric field, or parallel to the magnetic field, when viewed transverse to the field. When viewed parallel to the field direction the emission is unpolarized. The use of hydrogen has the unique characteristic that the Stark effect is linear with the electric field, producing a large spectral shift. For a magnetic field of 1.3 T and a beam energy of 55 keV, which are typical parameters for the Princeton Beta Experiment (PBX-M) tokamak,[6] the electric field on the atom is ~40 kV/cm. The average

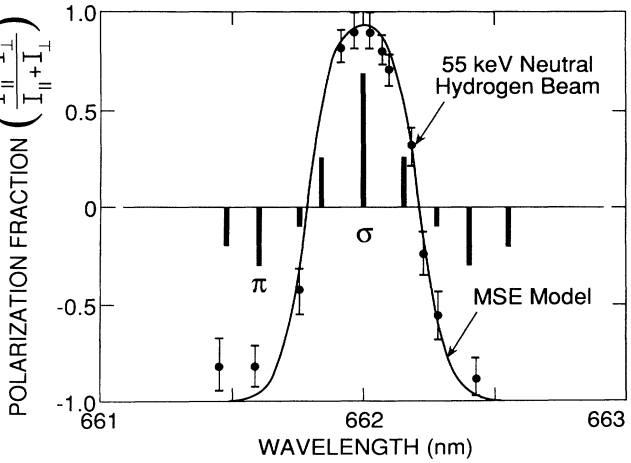

FIG. 1. The Stark-effect pattern of the Balmer-alpha (H_α) transition is shown by the vertical lines. The data points are from a spectral scan of the fractional polarization and the solid curve is numerically calculated.

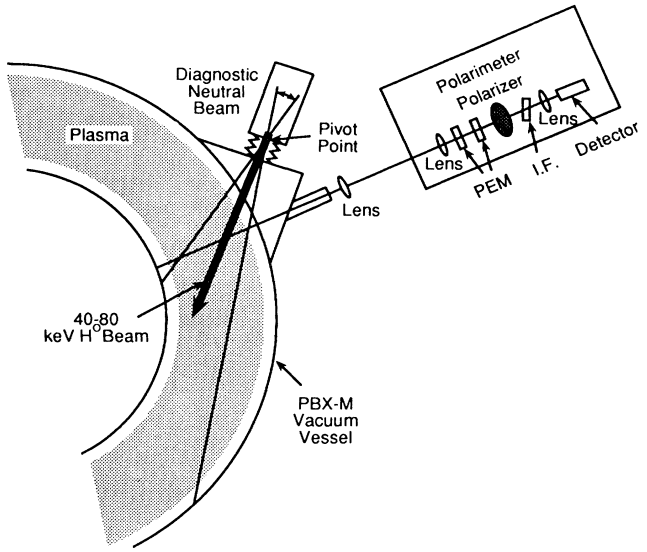

FIG. 2. Experimental setup of the diagnostic neutral beam and polarimeter on PBX-M.

spectral shift of the π lines for this field is ~ 4 Å. The Stark-effect pattern of the Balmer-alpha (H_α) lines showing the relative intensities and polarization from Ref. 5, along with a measurement of the polarization-fraction profile, is shown in Fig. 1. Each data point is a time average of 40 msec from a single PBX-M discharge. Also shown is a numerically computed fractional-polarization profile based on the convolution of the Stark shift and the filter profile.

The experimental apparatus for these measurements on PBX-M consists first of a highly collimated ($\sim 0.5°$) diagnostic neutral-hydrogen beam.[7] The energy can be varied from 40 to 80 keV, with a maximum injected power of ~ 40 kW in the full energy component. The beam power and energy for all the data shown here are 10 kW and 55 keV, respectively. The beam has a cross section of 5 cm vertically and 1.5 cm horizontally. The injection angle can be varied to change the radial intersection of the viewing cone with the beam, as shown in Fig. 2. The beam angle with respect to the optic axis of the instrumentation is typically 30°–40°. A lens collimates the collected light from the beam through the polarimeter and interference filter. The light is then focused onto a photomultiplier tube (PMT). The signal output from the PMT is amplified before going into a lock-in amplifier or waveform digitizer for later analysis. The interference filter has a spectral width of 4 Å, so as to transmit only the σ lines from the H_α spectra and thus maximize the polarization fraction. The filter can be tuned to different wavelengths by tilting it, which blue-shifts the passband. This is necessary for maximizing the signal and compensating for different Doppler shifts when the beam angle is changed, as during a radial scan.

The polarimeter uses a photoelastic modulator (PEM),[8,9] which is a birefringent crystal, such as quartz, with a piezoelectric transducer coupled to the crystal and driven at its resonant frequency (≤ 50 kHz). Because of the birefringence of the crystal, the transducer causes a time-varying phase shift of the electric field between the $\hat{\mathbf{x}}$ and $\hat{\mathbf{y}}$ directions through the crystal, which results in a rotation of the linearly polarized light. The rotation of the polarized light is converted to an amplitude modulation by the use of a fixed polarizer following the PEM's. The modulation amplitude of the light transmitted by the polarimeter can be proportional to either the sine or the cosine of the angle of polarization of the incident light, depending on its orientation with respect to the PEM. With two PEM's at slightly different frequencies and angles, both the sine and cosine of the angle of polarization can be measured. The transmitted intensity is

$$I \propto \sin(2\gamma)\cos(2\Omega_2 t) - \cos(2\gamma)\cos(2\Omega_1 t) + \cdots , \quad (1)$$

where γ is the angle of polarization and Ω_1 and Ω_2 are the resonant frequencies of the PEM's. Then the angle of the linearly polarized light equals the ratio of the signal amplitudes at the two PEM frequencies, $\tan(2\gamma) = I(2\Omega_2)/I(2\Omega_1)$. The two amplitudes, $I(2\Omega_2)$ and $I(2\Omega_1)$, can be determined in several ways, such as using Fourier analysis or a lock-in amplifier. Since only one channel is required, a single photomultiplier tube can be utilized for the detector.

An example of the H_α signal from the beam is shown in Fig. 3. The interference filter is set at ~ 6620 Å to compensate for the large Doppler shift from the beam emission. The signal intensity is estimated to be $\sim 5 \times 10^{12}$ photons/sec sr cm^2. The data shown have been smoothed with a running average over 1-msec time inter-

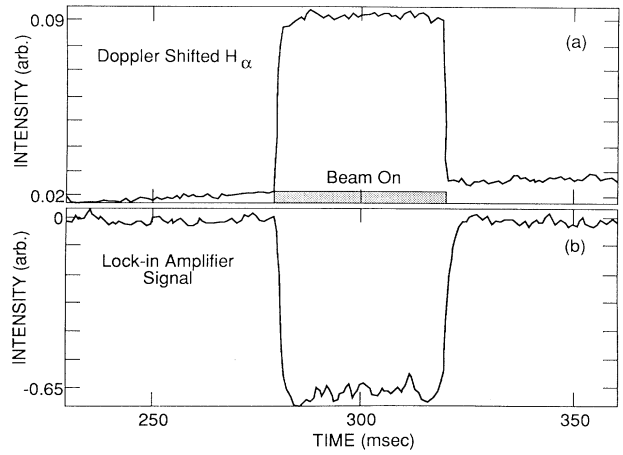

FIG. 3. (a) PMT and (b) lock-in amplifier signals from the neutral beam.

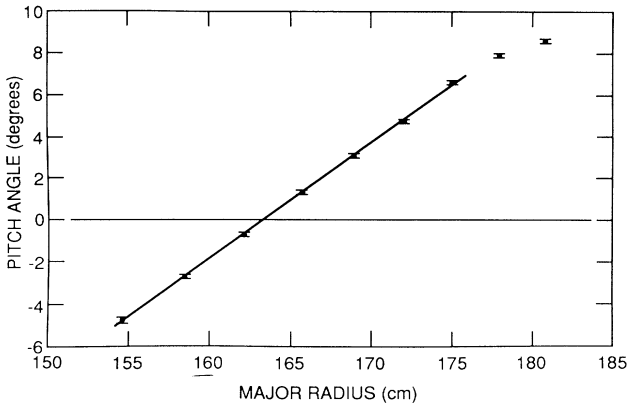

FIG. 4. Radial scan of the pitch angle.

vals to eliminate the high-frequency modulation from the polarimeter. The lock-in amplifier signal, with a 1-msec integration time constant, is also shown in Fig. 3, and it illustrates the signal modulation at the PEM resonant frequency.

As discussed earlier in the text, a shot-to-shot scan is required in order to obtain $q(r)$. This was done for an Ohmic discharge with a plasma current of 330 kA, major radius of 1.63 m, minor radius of 0.3 m, density of 3×10^{13} cm^{-3}, and toroidal field of 1.2 T. Only discharges where the plasma current was within 5% of 330 kA were used in the analysis to minimize shot-to-shot variations. The radial scan of the pitch angle is shown in Fig. 4. Each data point in the figure is a time average of 40 msec from three discharges. The uncertainty for each point is 0.1°, corresponding to $\sim$20 G. This was determined from a statistical analysis of the pitch-angle variation for many successive discharges. The safety factor at the magnetic axis, using the central seven points from the graph for the linear regression, is $q(0)_{\rm cyl}=0.63\pm0.02$ assuming a circular plasma. Systematic errors due to the beam and viewing geometry amount to an absolute error of $\sim\pm1$ cm. Also, the zero reference angle of the toroidal field with respect to the polarimeter axis, which is measured with beam injection into a gas-filled torus, introduces some error. However, both these errors cause a spatial shift in the data and do not contribute to the uncertainty in $q(0)_{\rm cyl}$. Systematic errors that do contribute to the $q(0)_{\rm cyl}$ uncertainty include the relative beam-viewing-geometry error, and the vertical displacement from the midplane of the plasma or the field of view. The contribution of these errors increases the uncertainty so that $q(0)_{\rm cyl}=0.63\pm0.03$, which illustrates the high precision obtainable with MSE polarimetry. For noncircular, low-β plasmas, such as those described here, $q(0)=\kappa q(0)_{\rm cyl}$, where κ is the elongation of a plasma with an elliptical cross section. This correction factor can be derived using the definition for $q(r)$ and the solution of the Grad-Shafranov equation for a noncircular cross section.[10] Based on results from an equilibrium code and measurements from an x-ray pin-hole camera, $\kappa=1.36\pm0.05$, which results in $q(0)=0.86\pm0.05$.

Independent confirmation of this value of $q(0)$ derived from the MSE polarimetry measurements has been obtained from two other $q(0)$ measurements on PBX-M for the same set of discharges. One technique uses an x-ray pin-hole camera, which can obtain an image of the plasma and determine the shape of the magnetic-flux surfaces in the plasma core.[11] The derived poloidal emissivity contours are compared with the poloidal flux contours calculated via a magnetics equilibrium code. This allows the elongation to be determined to within $\sim$4%. An assumed parametrization of the internal current distribution is adjusted, along with $q(0)$, to match the measured shape to determine the internal current distribution and $q(0)$. The measured electron pressure profiles and several external flux values are used to constrain the allowed equilibria. This procedure resulted in an axial safety factor of $q(0)=0.7\pm0.2$.

The Fast Ion Diagnostic Experiment (FIDE) is another technique for measuring plasma current profiles, and it has been demonstrated in two previous tokamak experiments.[12,13] A $q(0)$ of 0.8 ± 0.14, which represents an average over a sawtooth period, was obtained at 300 msec after the start of the discharge, and is in good agreement with the value from the MSE polarimetry diagnostic.

To consider but one of the many physics issues noted earlier in the text, many models describing sawtooth oscillations have been proposed. All these theories have different characteristics of the central $q(0)$ and the profile, $q(r)$. Measurements to date during discharges exhibiting sawtooth oscillations appear to indicate values of central $q(0)$ which are either significantly less than 1

(i.e., 0.7–0.9),[4,14,15] or close to unity.[2,15,16] These data are from a variety of machines, however, and recent attempts at measuring or inferring $q(0)$ on the same device have not yielded consistent results.[2,4,15] Measurements with MSE polarimetry on PBX-M have found $q(0)=0.86$ in an Ohmic plasma and $q(0)=0.77$ in a neutral-beam–heated plasma. For this reason, the present conclusion that $q(0)<1$, as determined by three independent techniques on PBX-M, has important implications for distinguishing between theoretical sawtooth models. In particular, it argues against those modes that require $q(0)$ to be very close to unity, such as the quasi-interchange model.[17] In addition, the measured $q(r)$ profile near the center of the plasma is flat out to about $a/3$ and well below unity. This is qualitatively different from the modified-Kadomtsev models[18,19] which require peaked or nonmonotonic profiles.

In conclusion, our definitive measurements have demonstrated that motional-Stark-effect polarimetry can yield accurate magnetic field pitch-angle profiles, and the technique is already being used to address important questions of plasma equilibrium and stability. Expected improvements in the design of the diagnostic and the neutral beam will yield an improved signal-to-noise ratio and time resolution. The technique also has the potential for multichannel capability to obtain $q(r,t)$ profile evolution during a single discharge. Data with this system have been obtained with densities of $\bar{n}_e=6\times10^{13}$ cm^{-3}, indicating this approach extrapolates favorably for use at higher densities and/or in larger machines.

The authors wish to thank M. Okabayashi and the PBX-M group for operation of the tokamak. This work was supported by the U.S. Department of Energy under Contracts No. DE-AC03-86ER80409 and No. DE-AC02-76-CHO-3073.

[1]F. DeMarco and S. E. Segre, Plasma Phys. **14**, 245 (1972).

[2]D. Wróblewski, L. K. Huang, and H. W. Moos, Phys. Rev. Lett. **61**, 1724 (1988).

[3]K. McCormick *et al.*, Phys. Rev. Lett. **58**, 491 (1987).

[4]W. P. West, D. M. Thomas, J. S. DeGrassie, and S. B. Zhang, Phys. Rev. Lett. **58**, 2758 (1987).

[5]E. U. Condon and G. H. Shortly, *The Theory of Atomic Spectra* (Cambridge Univ. Press, Cambridge, 1963).

[6]M. Okabayashi *et al.*, "Initial Results of the PBX-M Experiment," in Plasma Physics and Controlled Nuclear Fusion Research, 1988 (IAEA, Vienna, to be published).

[7]H. W. Kugel *et al.*, Nucl. Instrum. Methods (to be published).

[8]J. C. Kemp, J. Opt. Soc. Am. **59**, 950 (1969).

[9]J. C. Kemp, G. D. Henson, C. T. Steiner, and E. R. Powell, Nature (London) **326**, 270 (1987).

[10]J. P. Freidberg, *Ideal Magnetohydrodynamics* (Plenum, New York, 1987).

[11]R. J. Fonck *et al.*, Rev. Sci. Instrum. **59**, 1831 (1988).

[12]R. J. Goldston, Phys. Fluids **21**, 2346 (1978).

[13]D. D. Meyerhofer *et al.*, Nucl. Fusion **25**, 321 (1985).

[14]H. Soltwisch, Rev. Sci. Instrum. **59**, 1599 (1988).

[15]D. J. Campbell *et al.*, "Sawtooth Activity and Current Density Profiles in JET," in Plasma Physics and Controlled Nuclear Fusion Research, 1988 (IAEA, Vienna, to be published).

[16]H. Weisen, G. Borg, B. Joye, A. J. Knight, and J. B. Lister, Phys. Rev. Lett. **62**, 434 (1989).

[17]J. A. Wesson, Plasma Phys. Controlled Fusion **28**, 243 (1986).

[18]W. Park and D. A. Monticello, Princeton Plasma Physics Laboratory Technical Report No. PPPL-2601, 1989 (unpublished).

[19]R. G. Kleva, J. F. Drake, and R. E. Denton, Phys. Fluids **30**, 2119 (1987).